



Berner Fachhochschule
Haute école spécialisée bernoise
Bern University of Applied Sciences

Enhanced Physics-Based Models for State Estimation of Li-Ion Batteries

Master Thesis Presentation, August 19, 2020, MS Teams

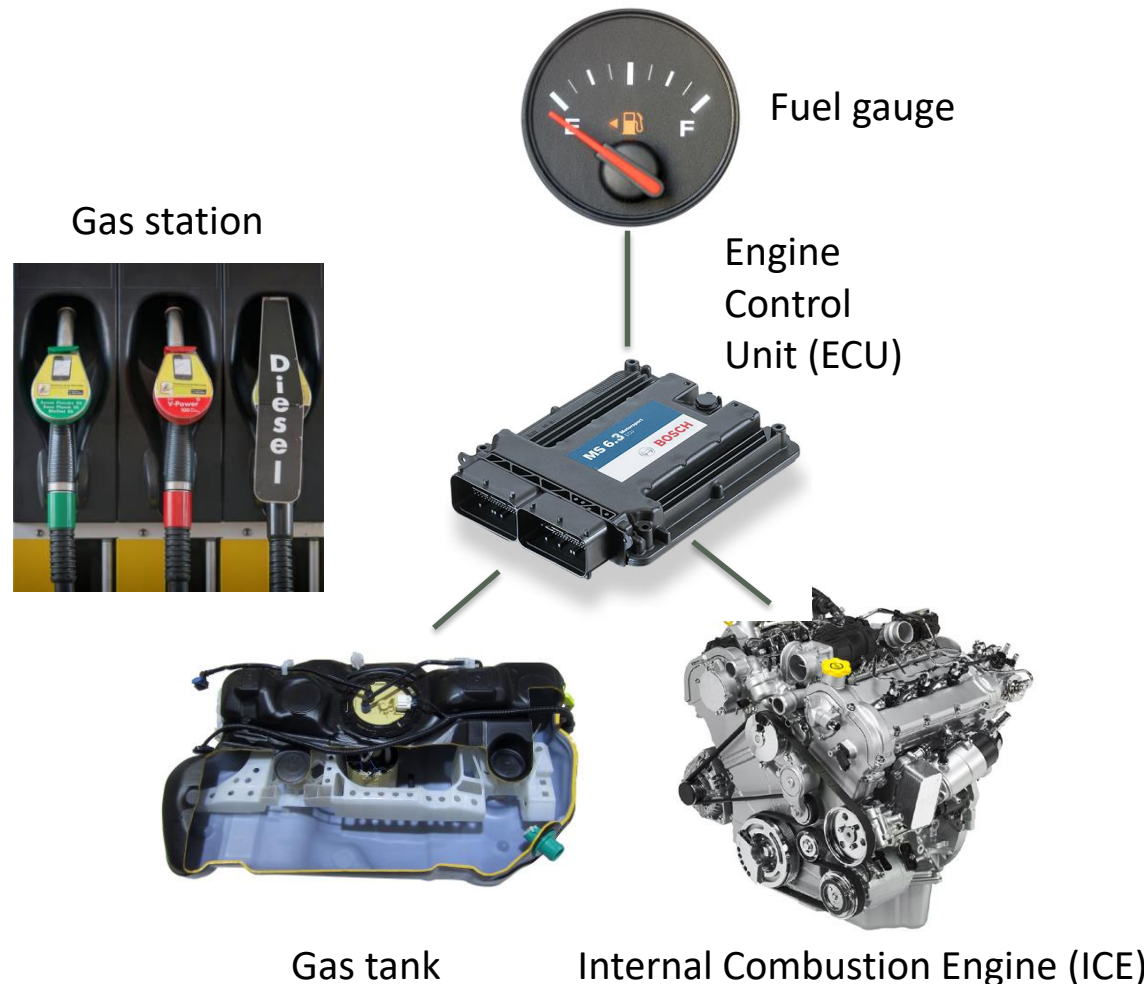
Author: Daniel Luder

Advisor: Prof. Dr. Andrea Vezzini, Dr. Priscilla Caliandro

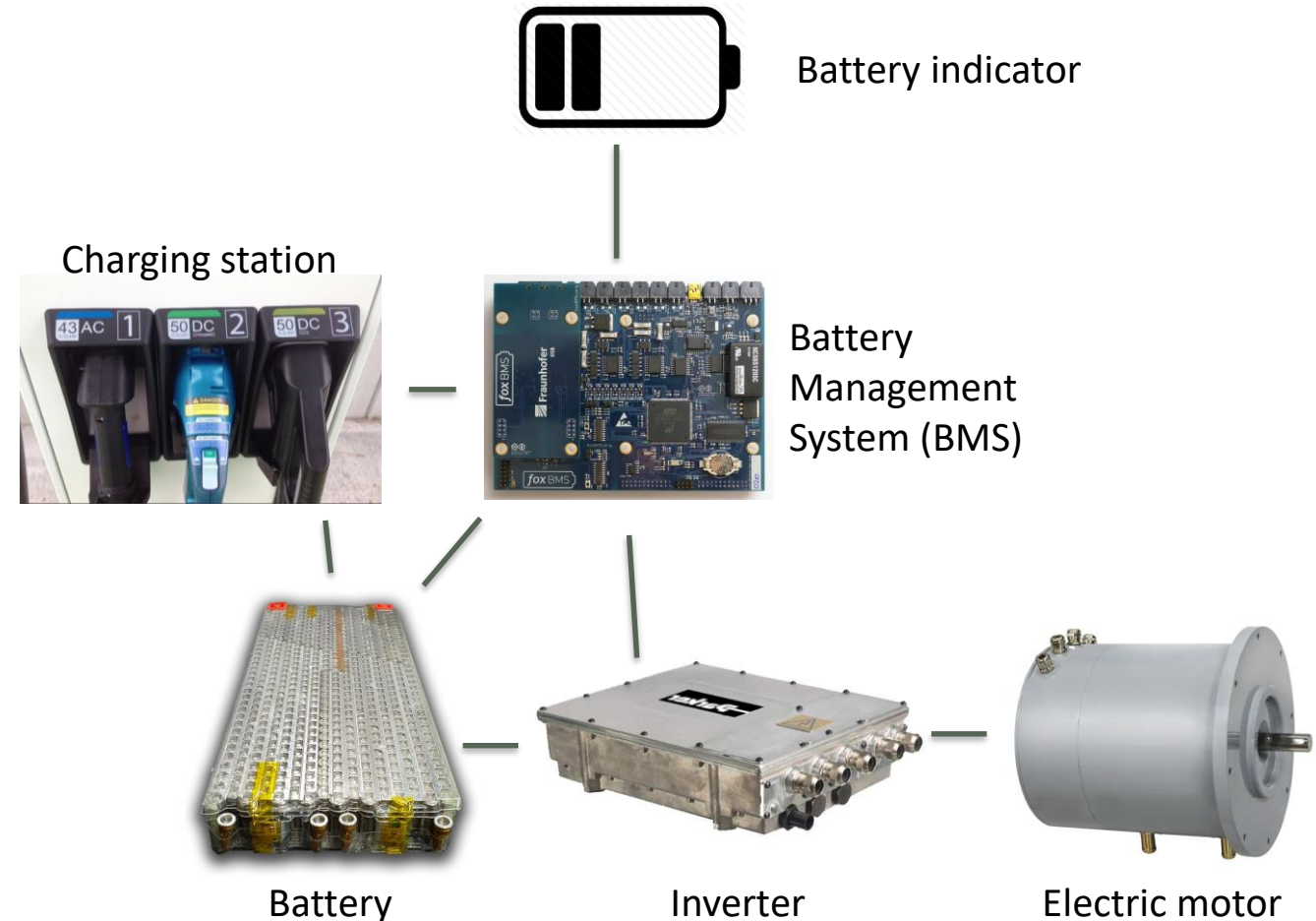
Expert: Dr. Corsin Battaglia (EMPA)

Motivation and Problem Description

Traditional (gasoline) vehicle



Battery Electric Vehicle (BEV)



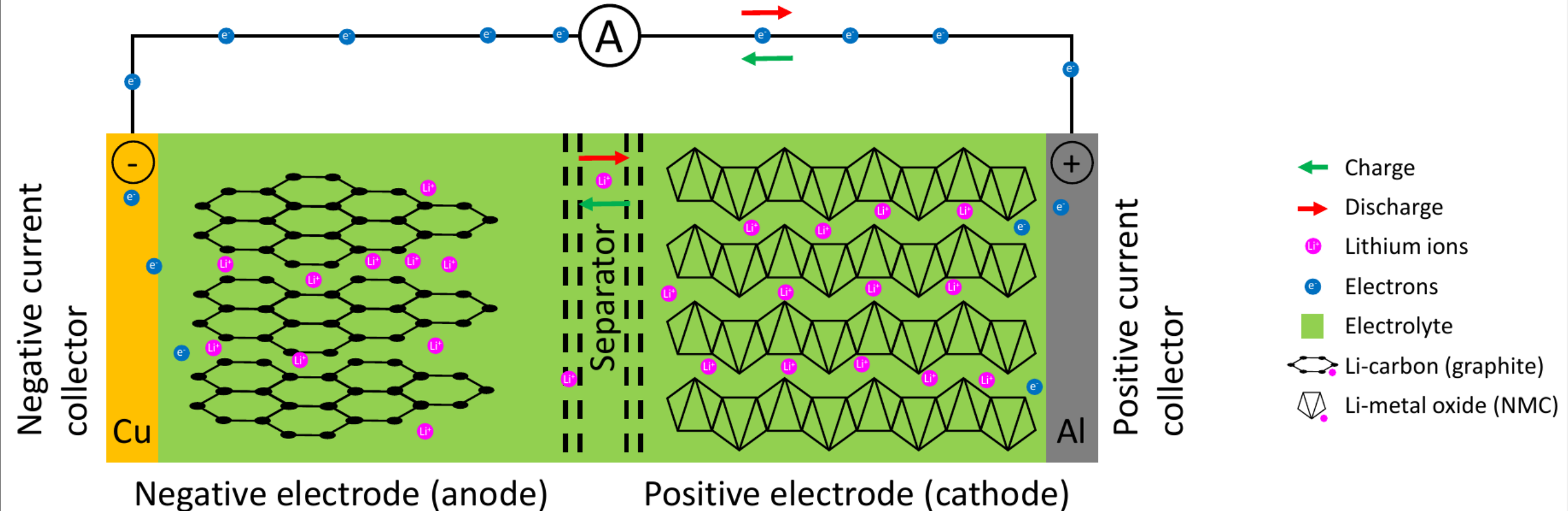
Research Objectives

- ▶ Implementation of a physics-based battery model
 - ▶ Detailed representation of electrochemical reactions and phenomena allowing:
 - ▶ Control degradation processes → prolong battery life
 - ▶ Calculate power limits → optimal/fast charging applications
 - ▶ Accurate voltage simulation → more precise state estimation
 - ▶ Meaningful state estimation
- ▶ Parameter identification of a commercial lithium-ion battery
- ▶ Simplification of the model towards implementation on an embedded system according to Model-Based Design (MBD)

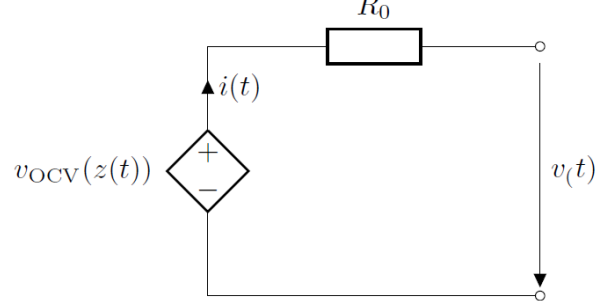
Lithium-Ion Batteries

State of Charge (SOC):
State of Health (SOH):

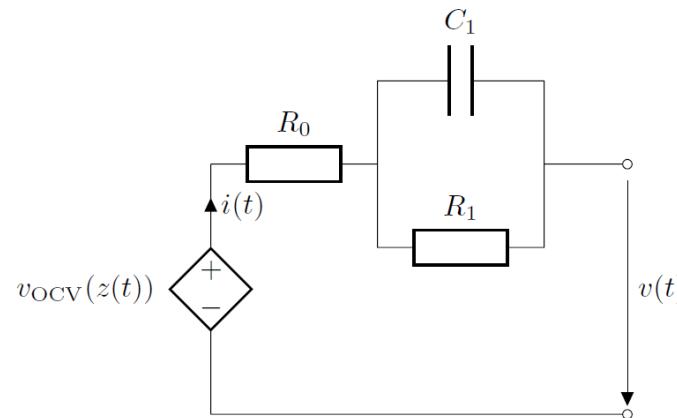
remaining charge [%]
capacity fade [%]



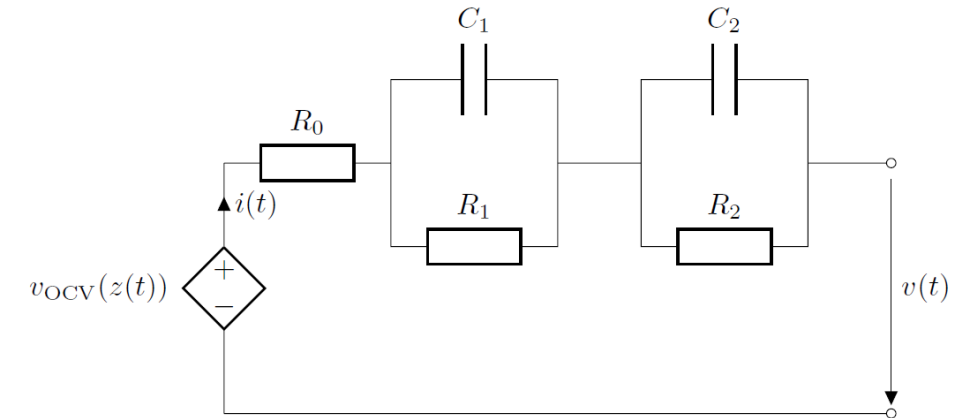
Equivalent Circuit Models (ECMs)



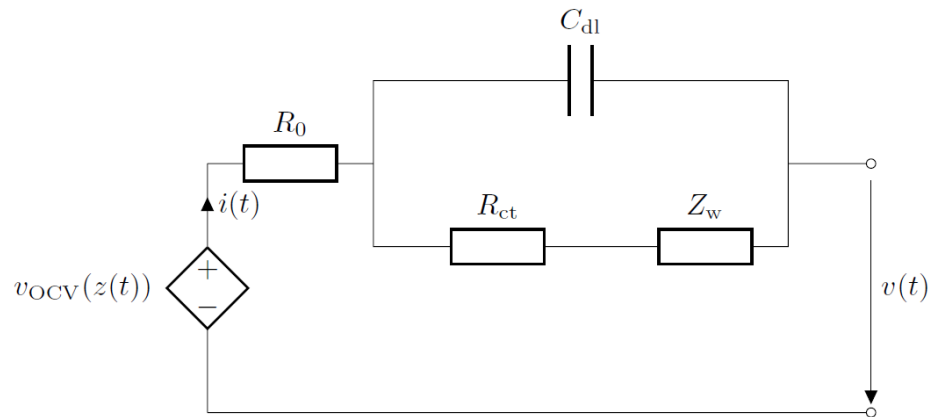
Rint model



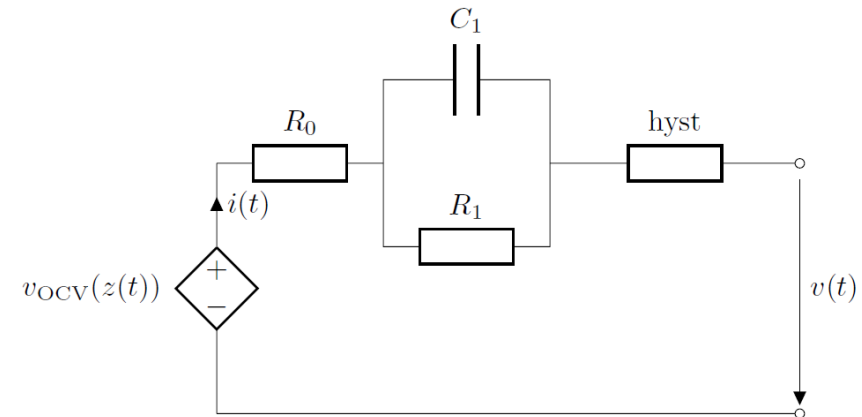
Thévenin model



Dual polarization model



Randles circuit model

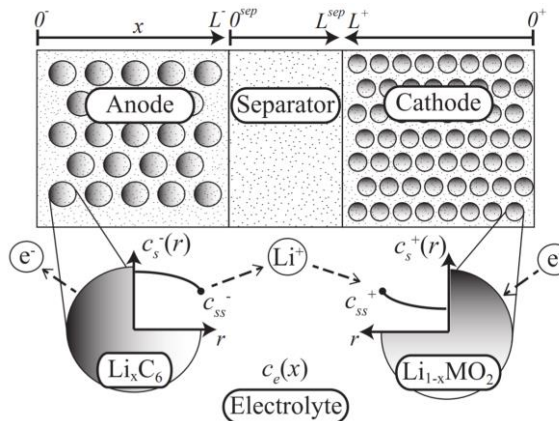
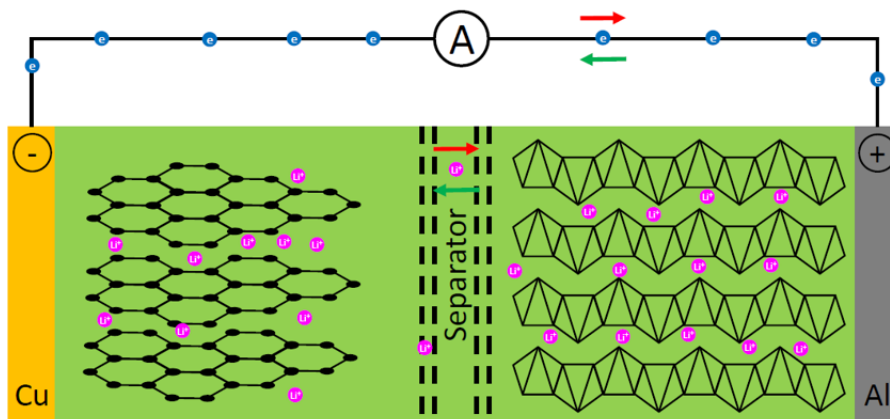


Enhanced Self-Correcting (ESC) battery model

Physics-Based Battery Models (PBMs)

Doyle-Fuller-Newman (DFN) battery model

- ▶ Pseudo-2D physics-based battery model
- ▶ Based on multiphase porous electrodes and concentrated solution theories
- ▶ Governed by a set of coupled nonlinear Partial Differential Equations (PDE)
 - ▶ Charge/mass conservation in the homogeneous solid/liquid phase
 - ▶ Electrochemical kinetics described by the Butler-Volmer equation



- Li concentration in the solid phase $c_s(x, r, t)$
- Li concentration in the liquid phase $c_e(x, t)$
- Electric potential in the solid phase $\Phi_s(x, t)$
- Electric potential in the liquid phase $\Phi_e(x, t)$
- Molar flux density at the solid/liquid interface $j(x, t)$

Sensitivity Analysis

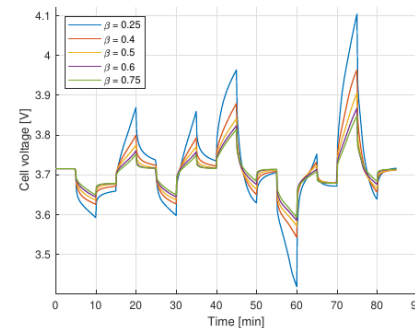
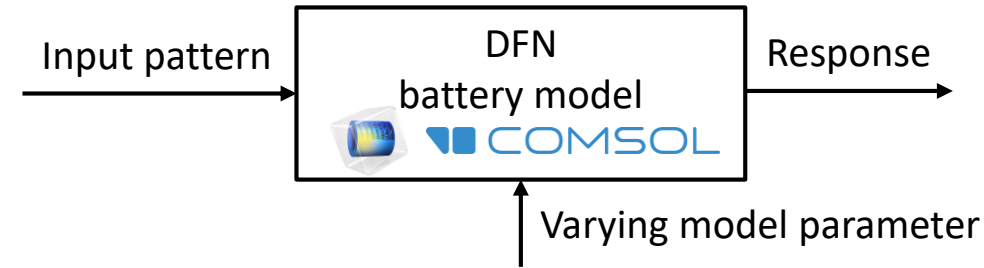
QR decomposition with column pivoting

- ▶ Identify the most sensitive parameter
- ▶ Scaling model parameters from literature
 - ▶ Linear, same order of magnitude
 - ▶ Logarithmic, different order of magnitude

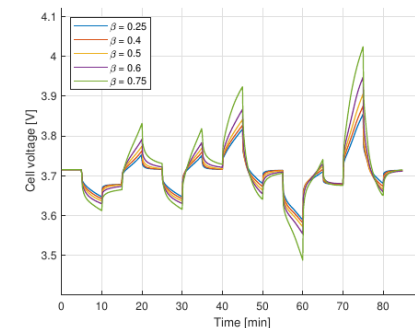
Sensitivity ranking	beta = 0.25	beta = 0.4	beta = 0.6	beta = 0.75	All betas
1st	rp_pos	rp_pos	Ds_pos	Ds_pos	rp_pos
2nd	rp_neg	eps_l_pos	rp_pos	i0ref_neg	Ds_pos
3rd	Ds_pos	Ds_pos	Ds_neg	rp_pos	i0ref_neg
4th	i0ref_neg	rp_neg	i0ref_neg	i0ref_pos	rp_neg
5th	eps_l_neg	cl_0	De	eps_l_neg	eps_l_neg
6th	eps_l_pos	De	cl_0	De	i0Ref_pos
7th	cl_0	t_plus	sigma_pos	eps_l_pos	eps_l_pos
8th	De	eps_l_neg	eps_l_neg	rp_neg	De
9th	Ds_neg	i0ref_pos	rp_neg	t_plus	Ds_neg
10th	i0ref_pos	i0ref_neg	eps_l_sep	Ds_neg	cl_0
11th	eps_l_sep	eps_l_sep	eps_l_pos	cl_0	t_plus
12th	sigma_pos	sigma_pos	i0ref_pos	sigma_pos	sigma_pos
13th	t_plus	Ds_neg	t_plus	eps_l_sep	eps_l_sep



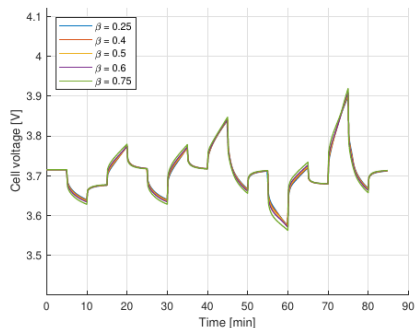
Geometric parameter



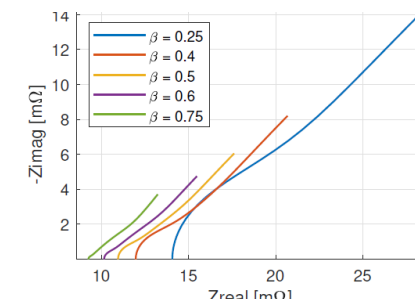
1st most sens.



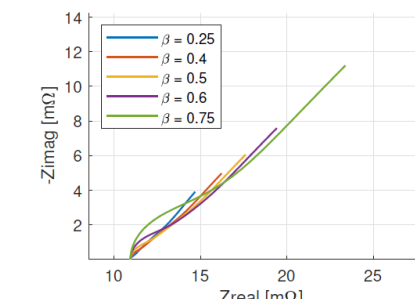
2nd most sens.



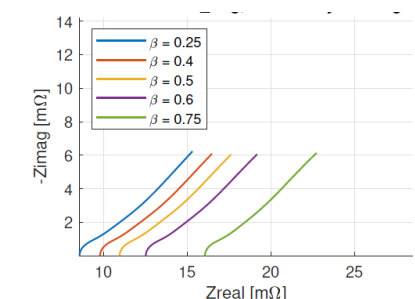
3rd most sens.



1st most sens.



2nd most sens.

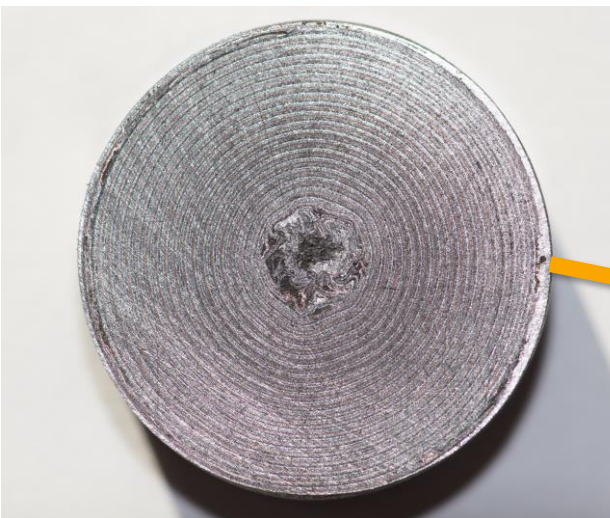


3rd most sens.

Microstructure Analysis – Sample Preparation



Unrolled battery jelly roll



Cut battery jelly roll



Vacuum impregnation



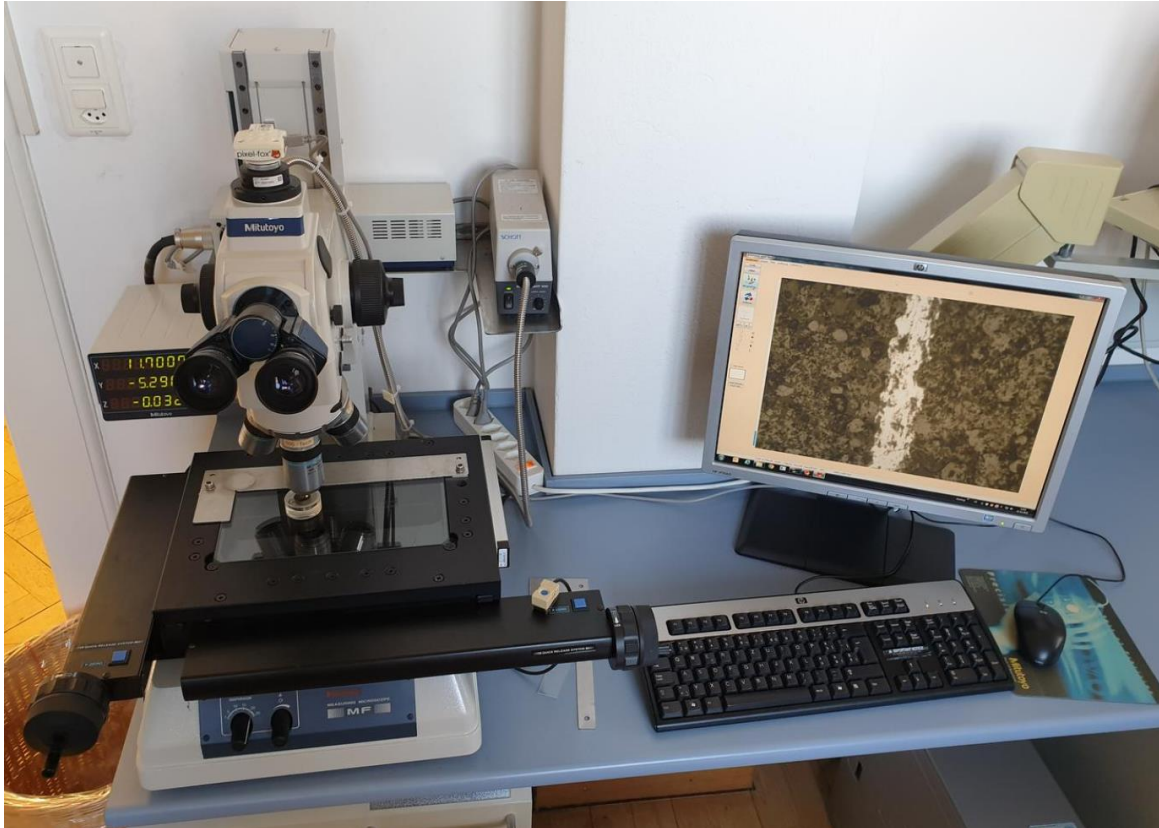
Grinding machine



Polishing machine

Microstructure Analysis – Optical microscope

Optical microscope



Optical microscope to measure the layer thickness



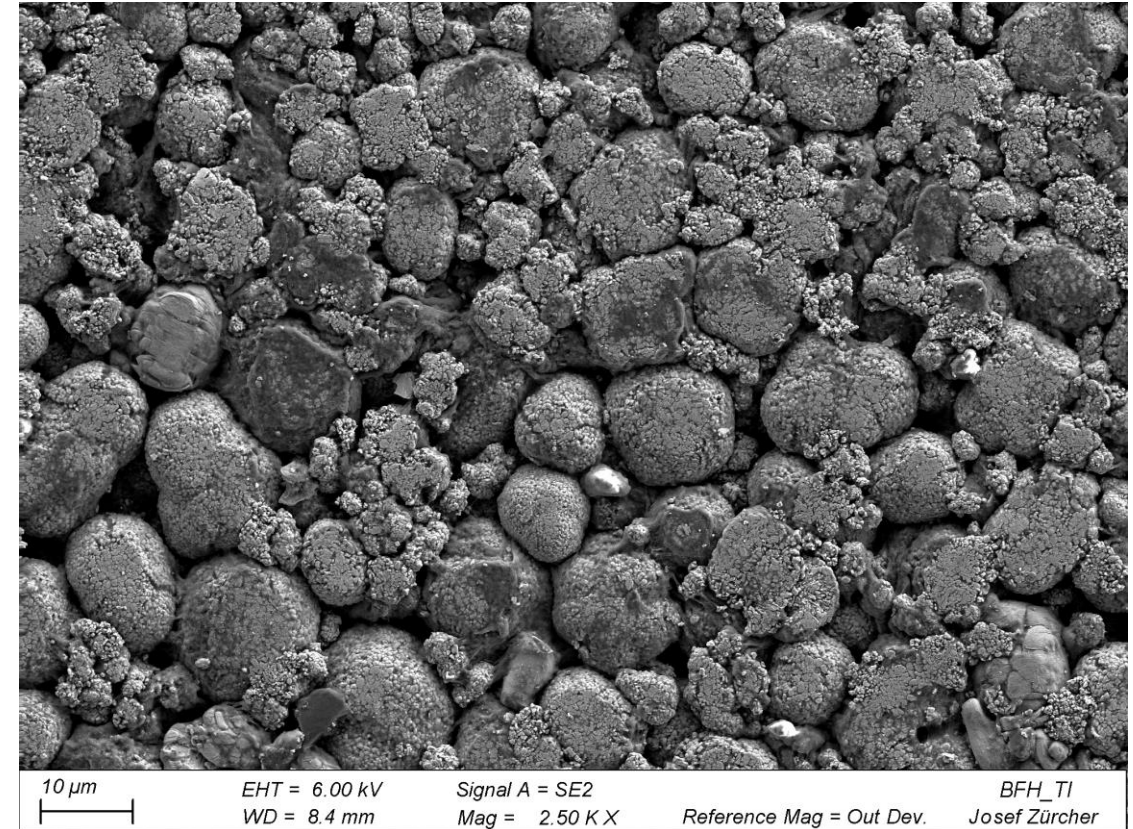
View of the jelly roll design

Microstructure Analysis – Scanning Electron Microscope (SEM)

Scanning Electron Microscope (SEM)



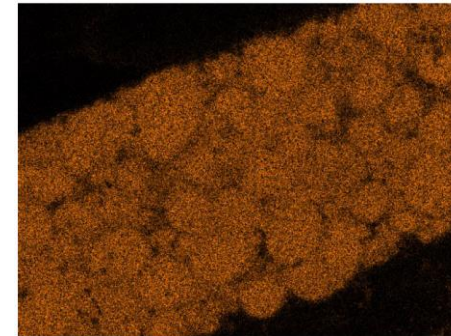
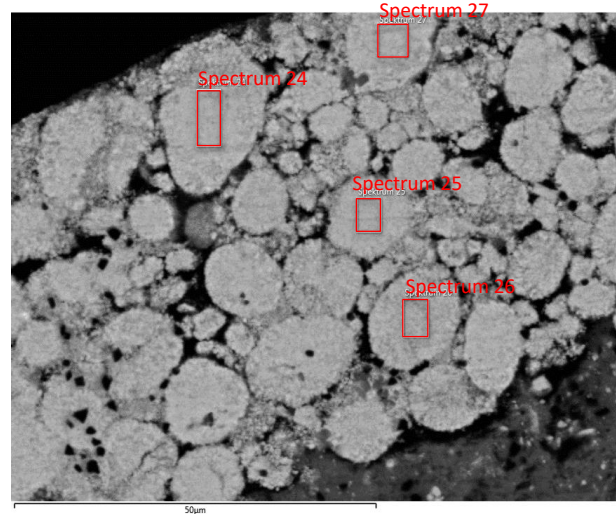
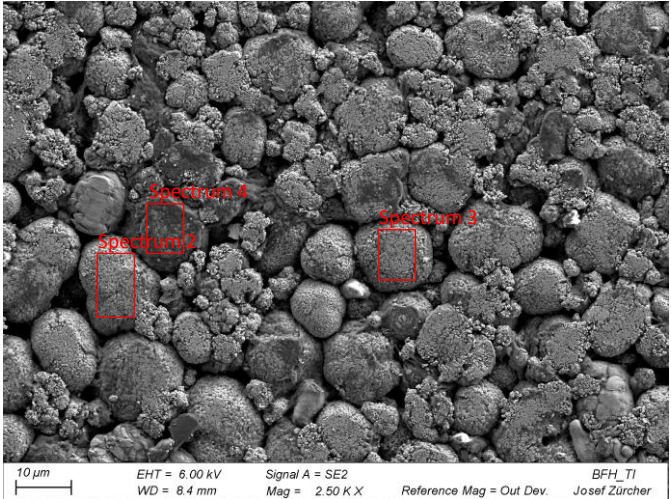
Scanning Electron Microscope (SEM) used for the microstructure analysis



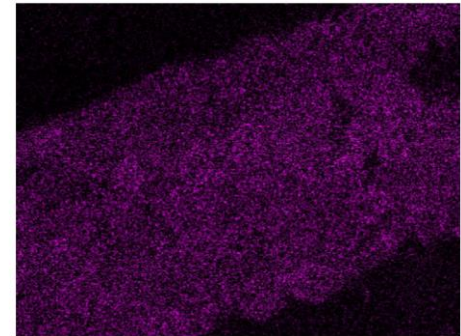
SEM image of the coated cathode material of the unrolled jelly roll

Microstructure Analysis – Scanning Electron Microscope (SEM)

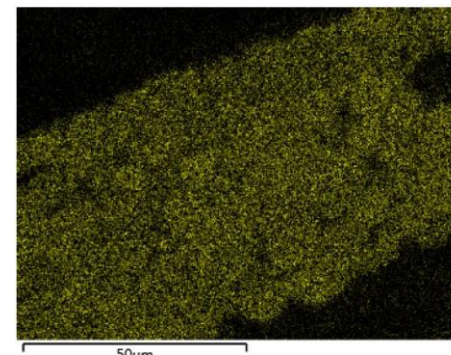
Energy Dispersive X-Ray Spectroscopy (EDX)



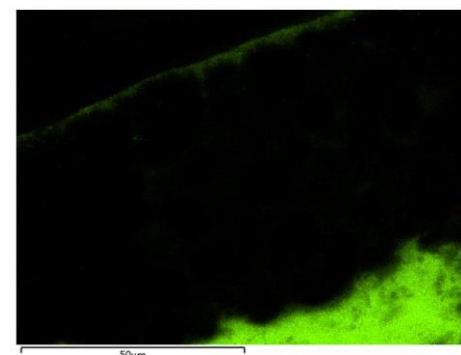
(a) Ni



(b) Mn



(c) Co



(d) Al

EDX mapping analysis

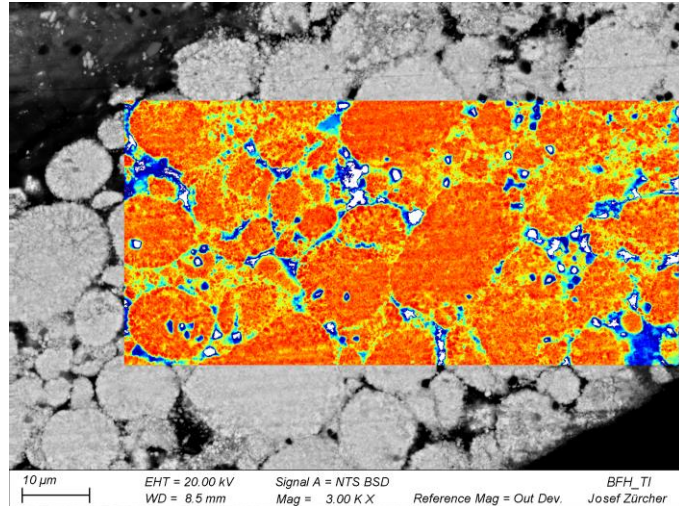
Spectrum name	Ni [wt%]	Mn [wt%]	Co [wt%]	Total [wt%]
Spectrum 2	82.50	4.95	12.55	100
Spectrum 3	82.19	5.18	12.62	100
Spectrum 4	82.63	4.94	12.43	100
Spectrum 24	86.57	2.97	10.46	100
Spectrum 25	83.09	4.45	12.46	100
Spectrum 26	83.89	4.06	12.05	100
Spectrum 27	86.49	3.13	10.38	100



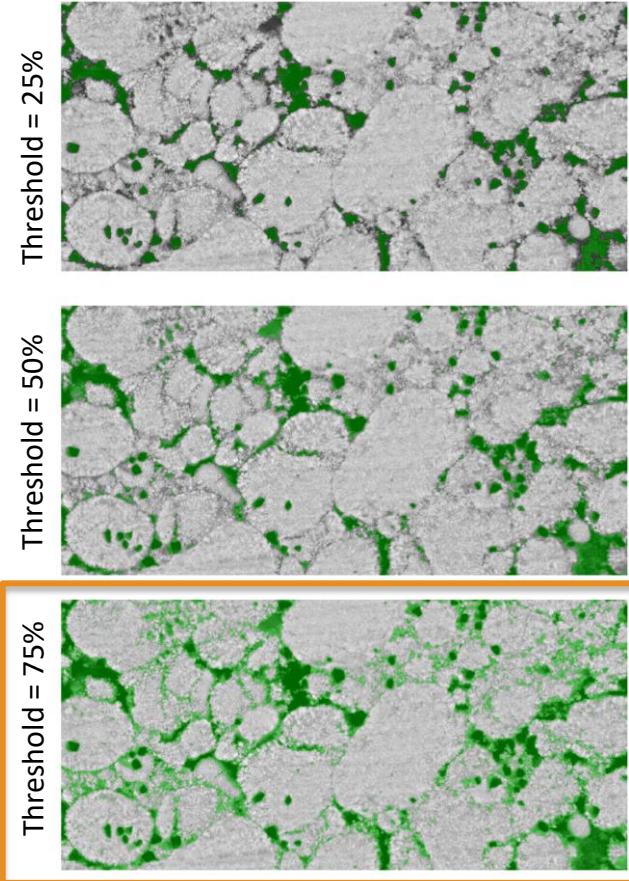
Nickel-rich cathode (NMC811)
Silicon graphite anode (SiC)

Microstructure Analysis – Image Processing

Determine porosity and volume fraction of the positive electrode



SEM image



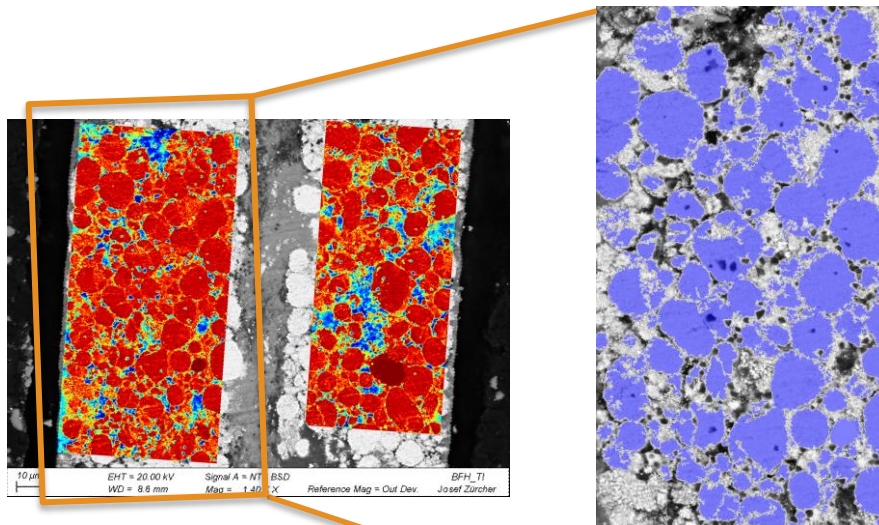
Otsu's multilevel binary threshold

Location	Active volume fraction		
	Threshold = 25%	Threshold = 50%	Threshold = 75%
Sample 1 left	93.6%	85.8%	74.4%
Sample 1 right	92.2%	83.8%	72.1%
Sample 2 top	91.0%	81.8%	68.2%
Sample 2 bottom	93.4%	85.5%	72.9%
Sample 3	93.7%	88.2%	75.7%
Sample 4 top	91.3%	83.3%	68.7%
Sample 4 bottom	89.4%	80.1%	64.3%

Most likely active volume fraction

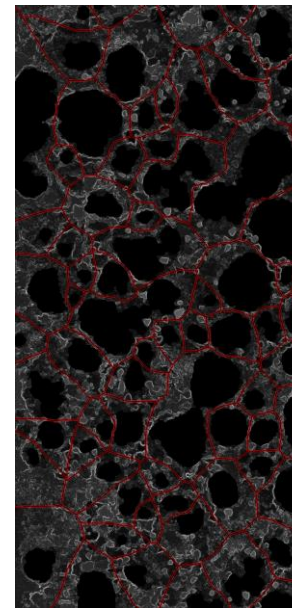
Microstructure Analysis – Image Processing

Determine the particle size of the positive electrode

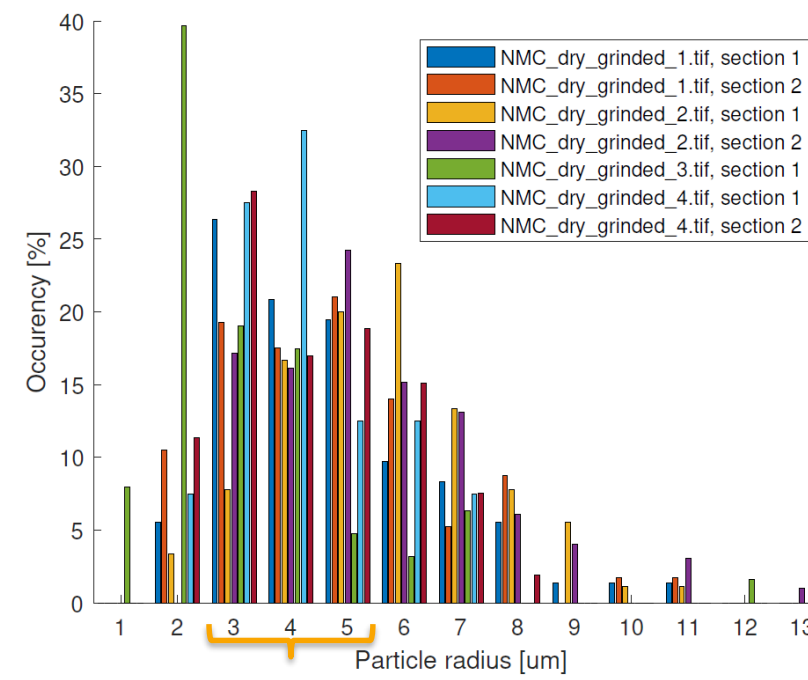
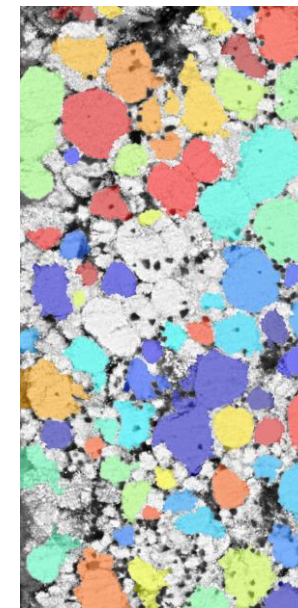


SEM image

Binarization and
Morphological
operations

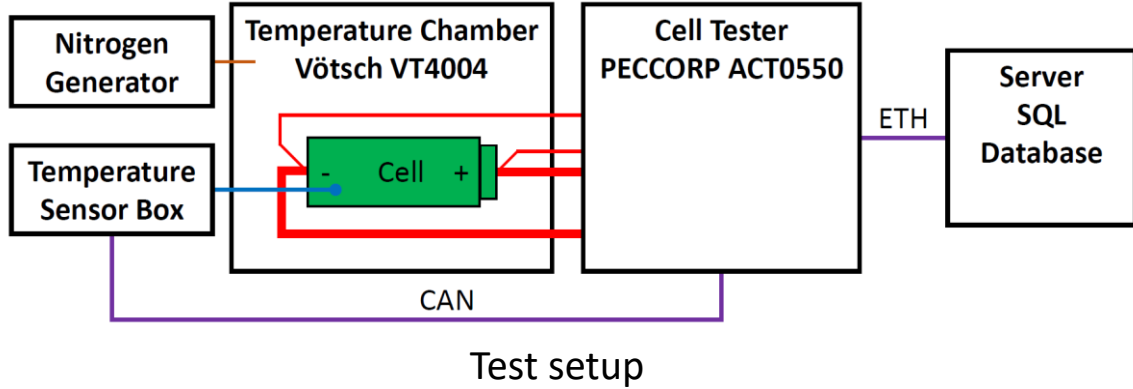


Watershed and Skeleton by
Influence Zones (SKIZ)

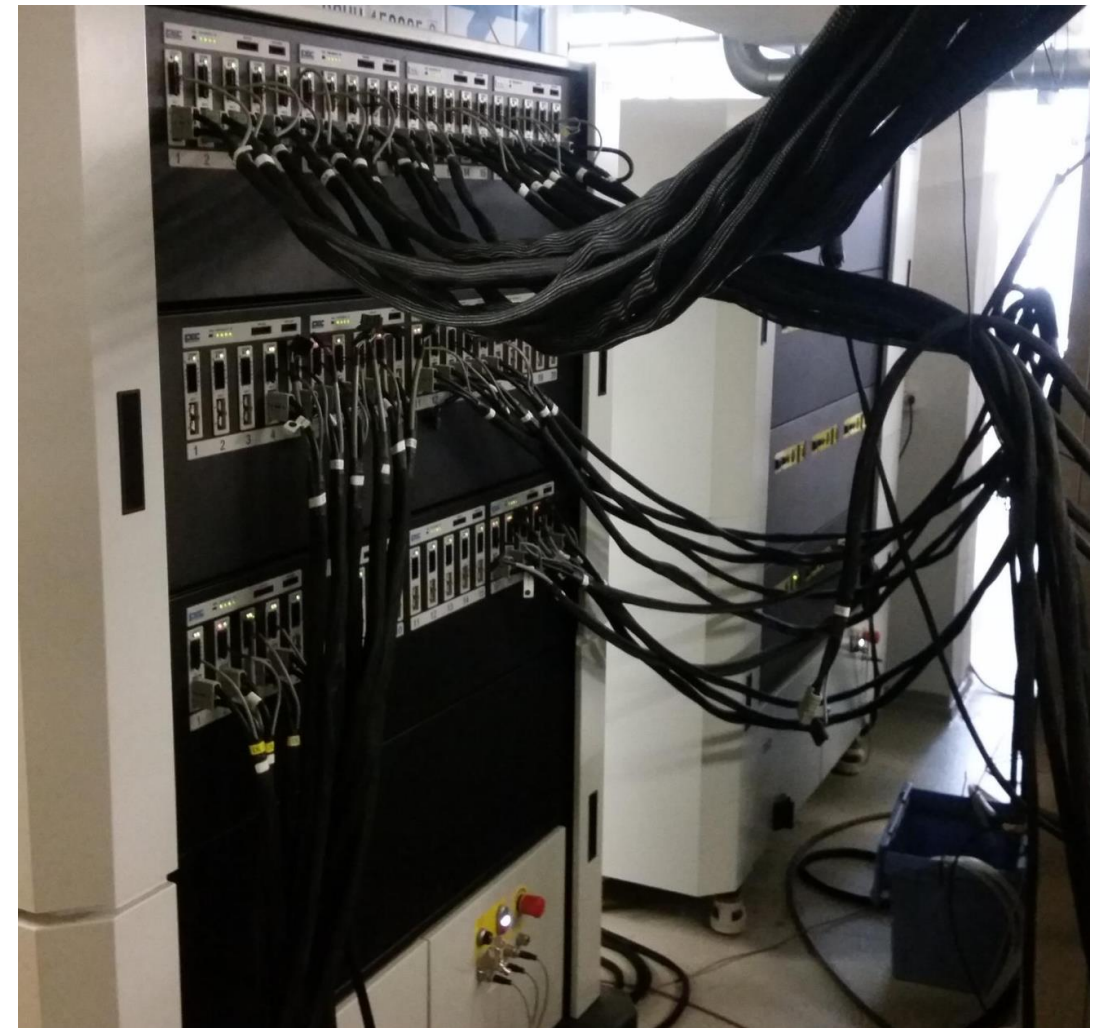


Most likely particle radius

Lithium-Ion Battery Testing



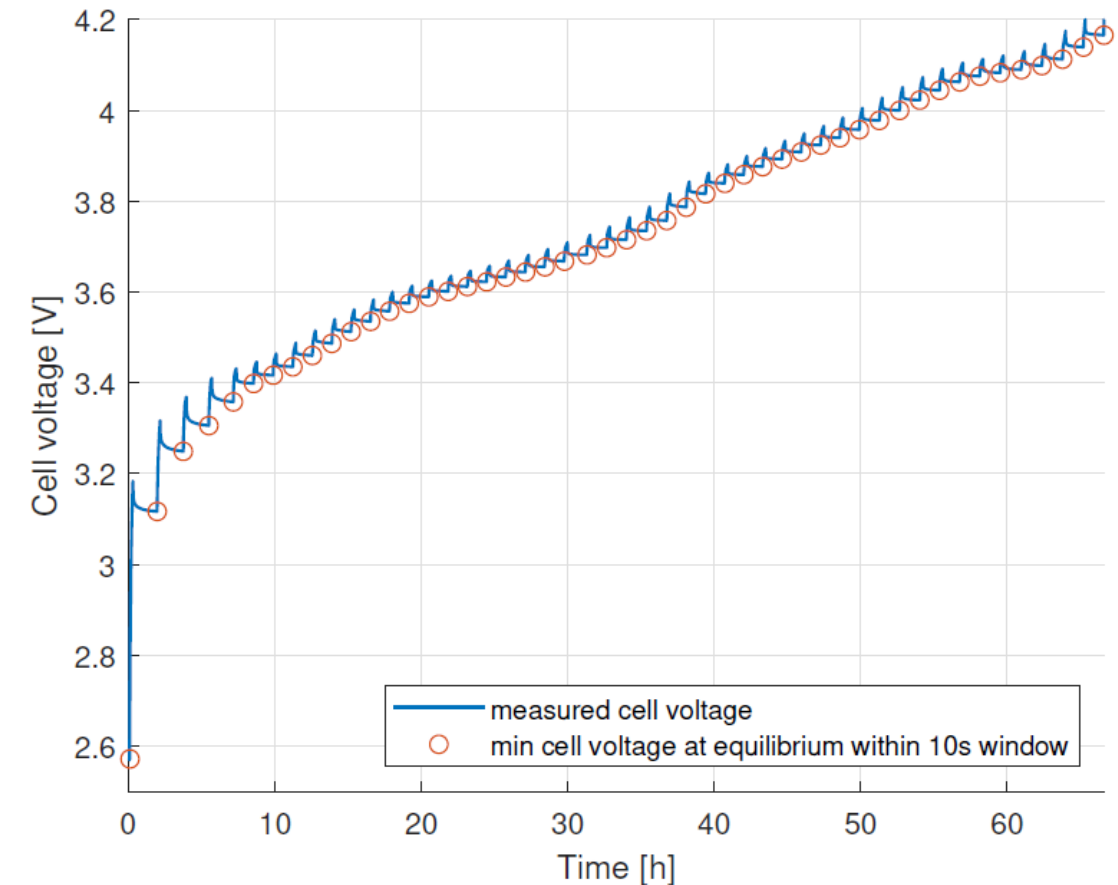
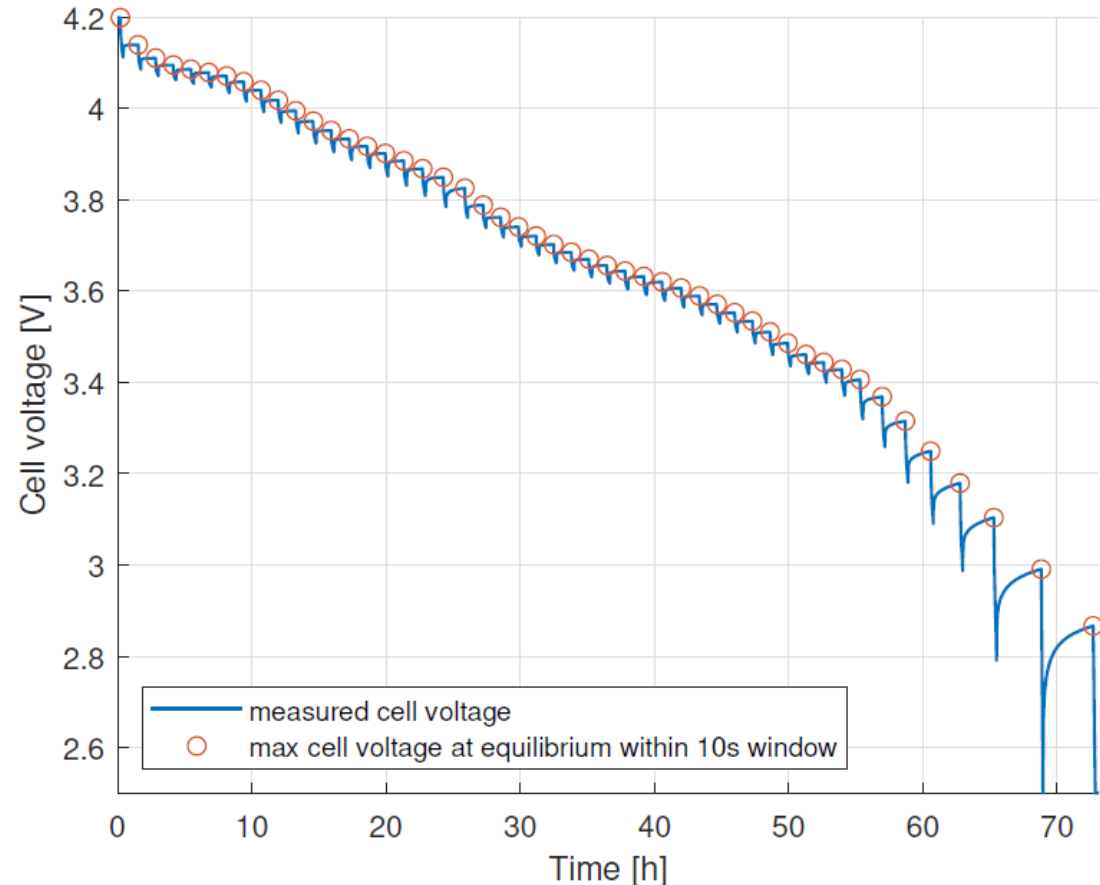
Cells in the temperature chamber



Cell tester ACT0550

Parameter Identification by Model Optimization

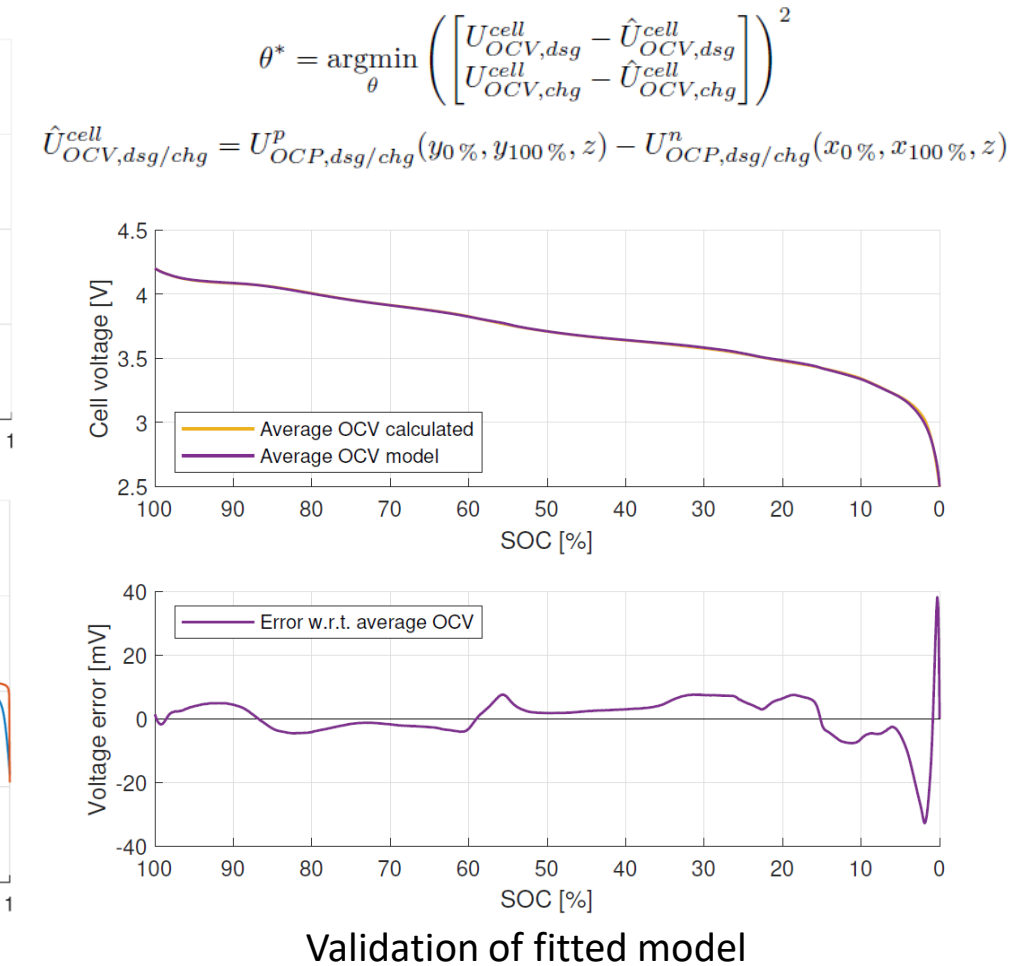
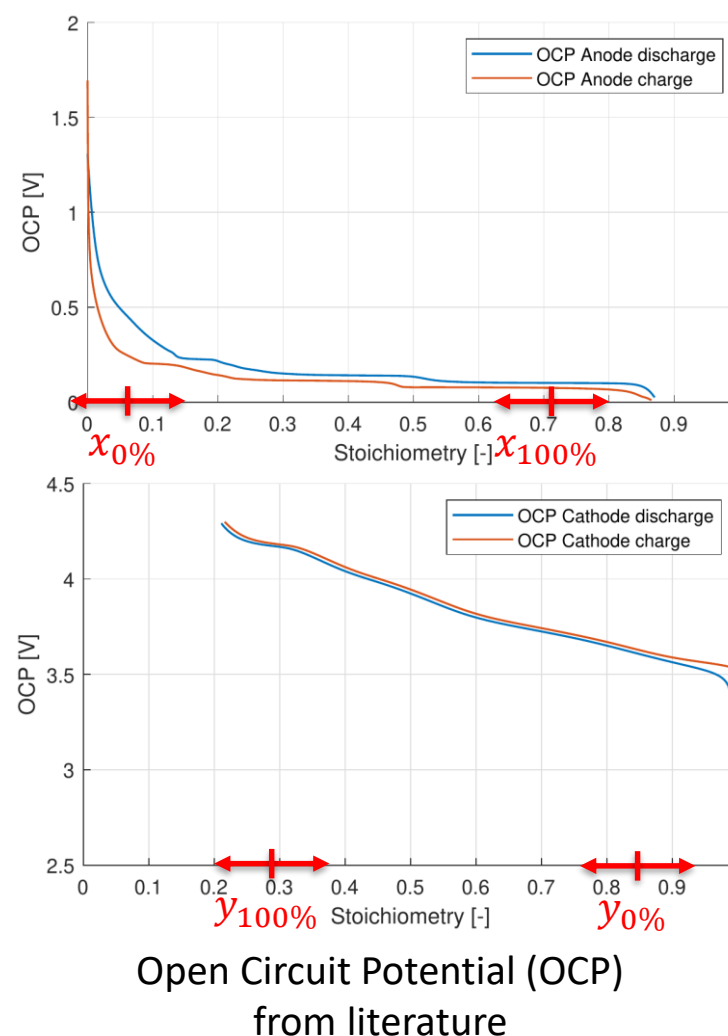
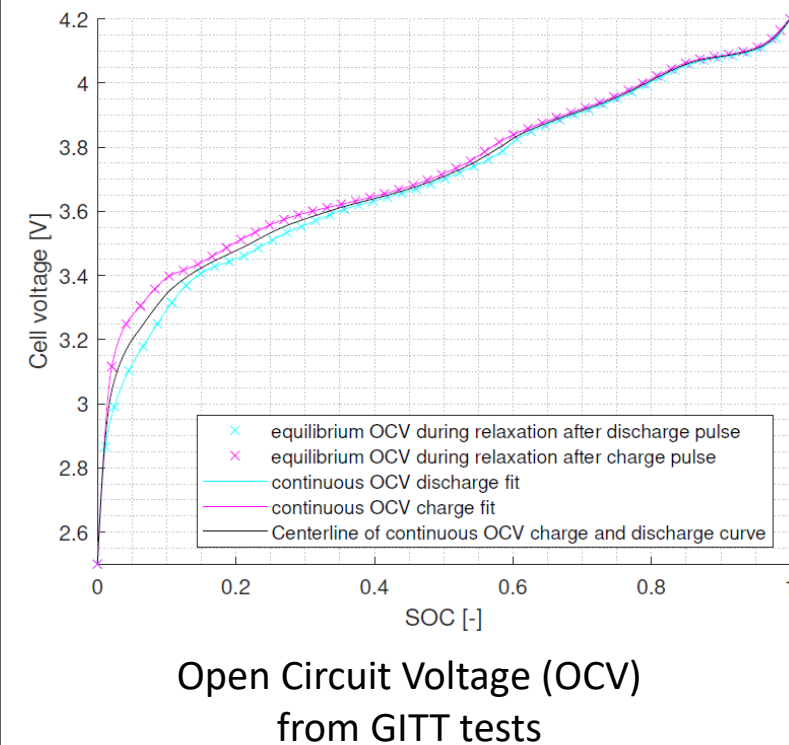
Determine the thermodynamic model parameters



Improved Galvanostatic Intermittent Titration Technique (GITT) test

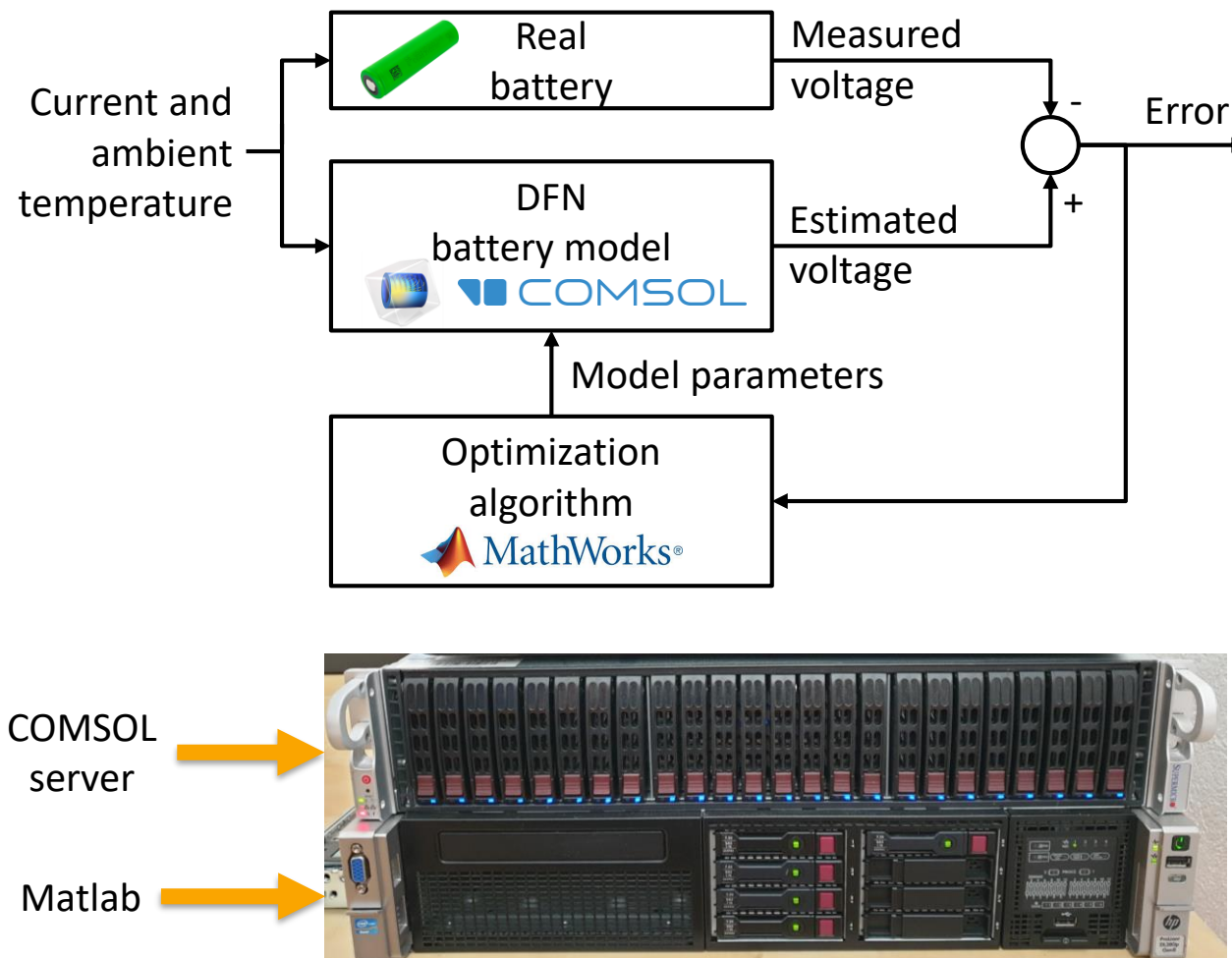
Parameter Identification by Model Optimization

Determine the thermodynamic model parameters



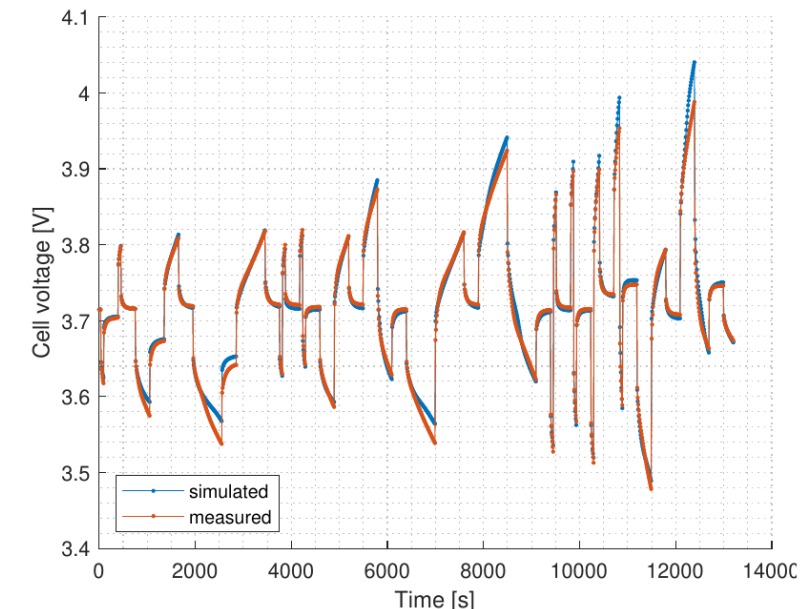
Parameter Identification by Model Optimization

Determine the kinetic model parameters



$$\hat{\mathbf{p}} = \underset{\mathbf{p}}{\operatorname{argmin}} \|\mathbf{f}(\mathbf{p}, \mathbf{I}_{\text{app}}(t))\| = \underset{\mathbf{p}}{\operatorname{argmin}} \left(\begin{bmatrix} f_1(\mathbf{p}, I_{1,\text{app}}(t)) \\ f_2(\mathbf{p}, I_{2,\text{app}}(t)) \\ \vdots \\ f_n(\mathbf{p}, I_{n,\text{app}}(t)) \end{bmatrix} \right)^2$$

$$f_i(\mathbf{p}, I_{i,\text{app}}(t)) = V_{\text{model}}(\mathbf{p}, I_{i,\text{app}}(t)) - V_{\text{cell}}(\mathbf{p}, I_{i,\text{app}}(t))$$

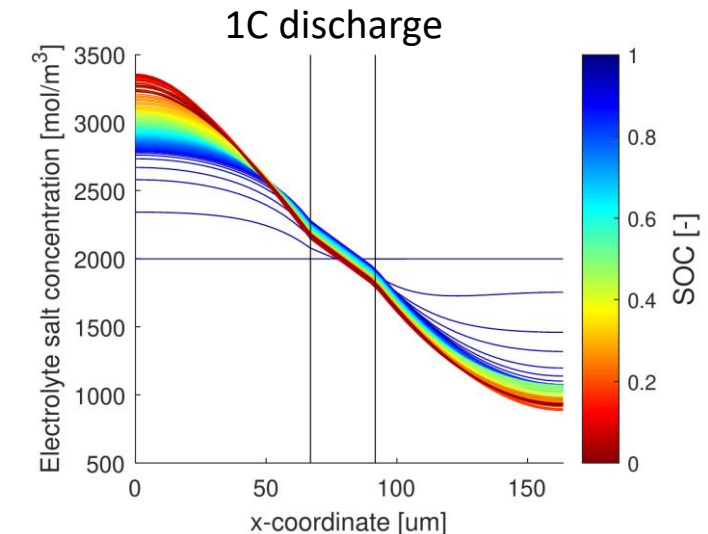
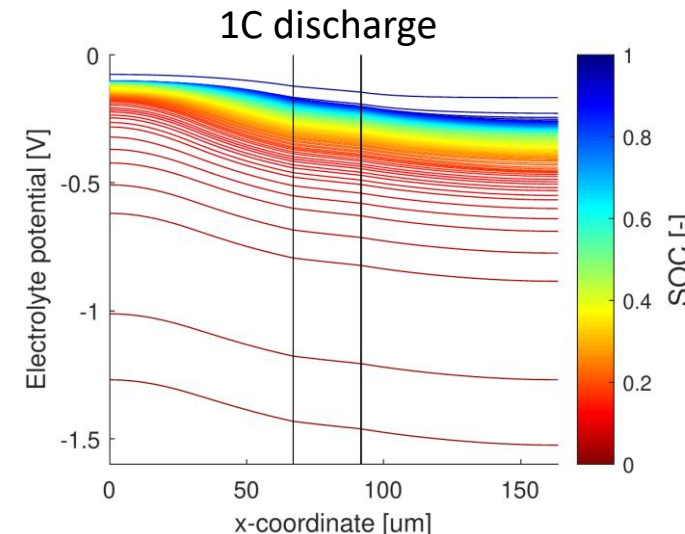
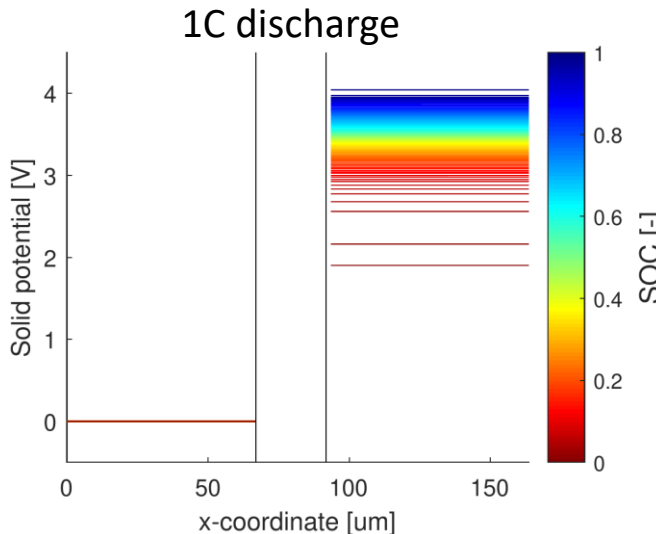
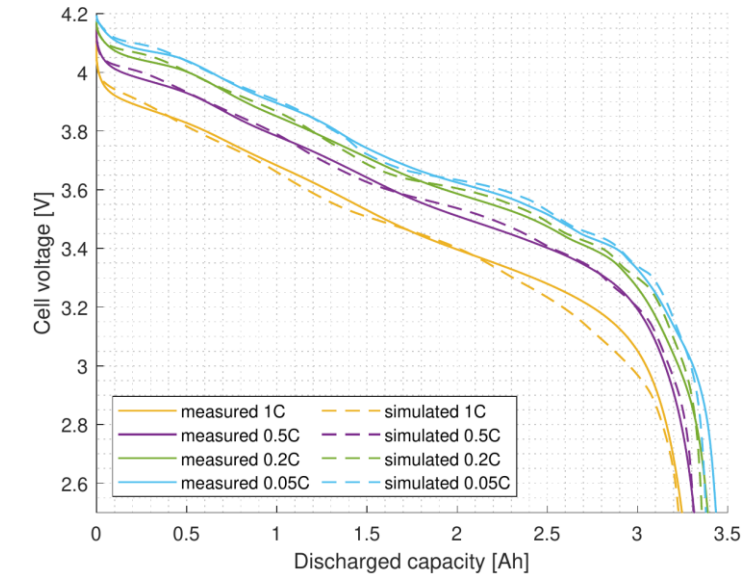


Doyle-Fuller-Newman (DFN) Model Validation

Constant Current (CC) discharge tests

- Li concentration in the solid phase $c_s(x, r, t)$
- Li concentration in the liquid phase $c_e(x, t)$
- Electric potential in the solid phase $\Phi_s(x, t)$
- Electric potential in the liquid phase $\Phi_e(x, t)$
- Molar flux density at the solid/liquid interface $j(x, t)$

Performance of
the DFN model
for different CC
discharges



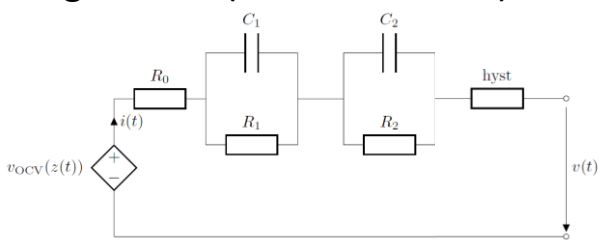
Doyle-Fuller-Newman (DFN) Model Validation

Standardized Drive Cycles

Enhanced Self-Correcting battery model

Average RMSE (90% - 10% SOC): 22.2mV

Average RMSE (90% - 20% SOC): 16.2mV



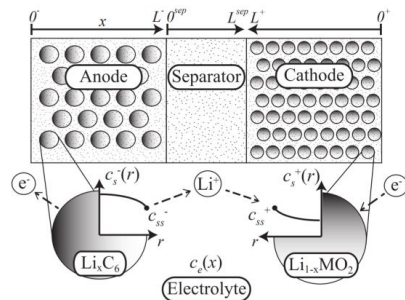
Enhanced model (2RC elements)	Drive Cycle	C-rate [C]	SOC [%]								
			90	80	70	60	50	40	30	20	10
HWFET	2C		9.3	14.5	17.5	27.8	10.0	12.8	11.3	14.3	63.4
NYCC	2C		16.8	17.2	17.8	20.2	16.8	17.4	16.8	17.7	26.4
UDDS	2C		11.3	15.4	16.1	29.7	13.1	14.5	14.3	18.5	51.2
US06	2C		8.7	13.2	17.2	25.5	9.6	11.2	10.3	10.7	74.9
HWFET	5C		12.2	10.4	14.4	15.4	10.3	8.8	8.6	25.1	137.0
NYCC	5C		13.9	16.3	17.8	23.6	14.7	16.1	14.7	17.5	41.6
UDDS	5C		9.9	11.3	14.8	25.4	9.4	10.4	9.6	11.5	94.0
US06	5C		39.3	22.5	23.2	23.8	25.6	19.2	18.8	26.5	69.6

RMSE for the Enhanced Self-Correcting battery model in mV

Doyle-Fuller-Newman battery model

Average RMSE (90% - 10% SOC): 17.3mV

Average RMSE (90% - 20% SOC): 11.4mV



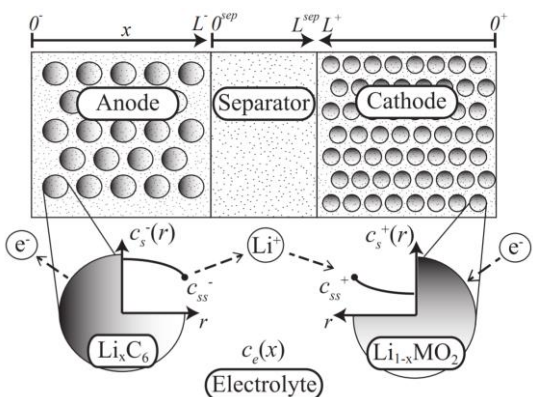
Doyle-Fuller-Newman battery model	Drive Cycle	C-rate [C]	SOC [%]								
			90	80	70	60	50	40	30	20	10
HWFET	2C		7.5	11.2	12.2	17.2	4.7	13.8	6.7	13.8	64.5
NYCC	2C		1.7	2.3	2.6	4.0	1.6	3.4	0.9	2.6	13.1
UDDS	2C		6.1	6.8	6.9	17.9	3.0	8.6	4.1	12.1	52.3
US06	2C		10.5	15.5	16.8	15.9	7.1	17.1	7.9	14.8	74.3
HWFET	5C		6.3	26.0	15.7	8.9	19.1	24.4	8.9	13.5	142.9
NYCC	5C		4.3	5.4	7.1	11.8	2.5	7.2	2.8	6.9	33.8
UDDS	5C		18.1	16.0	12.9	11.2	7.9	17.2	11.9	16.2	95.0
US06	5C		21.7	27.9	15.8	9.2	37.1	21.7	10.3	23.8	43.5

RMSE for the Doyle-Fuller-Newman battery model in mV

Single Particle Model (SPM) with electrolyte dynamics

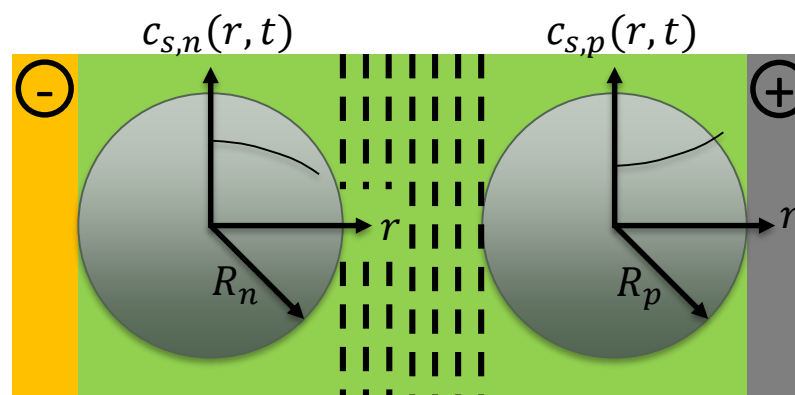
Simplification of the Doyle-Fuller-Newman (DFN) battery model

- Partial Differential Equation (PDEs)
- Computational complex



Doyle-Fuller-Newman (DFN)

- Approximates the solid phase of each electrode with a single spherical particle



Single Particle Model (SPM)
with electrolyte dynamics

- Approximate microscale diffusion inside porous electrodes by a polynomial
- Apply volume averaging methods

$$\frac{d}{dt} \bar{c}_s(t)$$

$$\frac{d}{dt} \bar{q}_s(t)$$

$$\frac{d}{dt} \bar{c}_e(t)$$

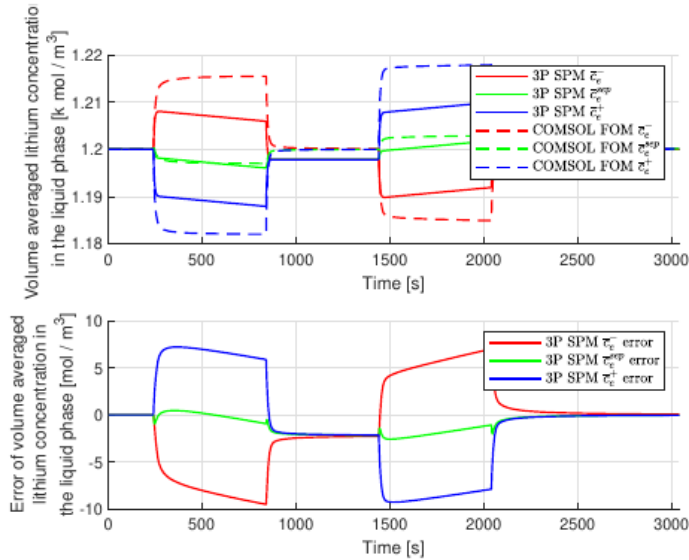
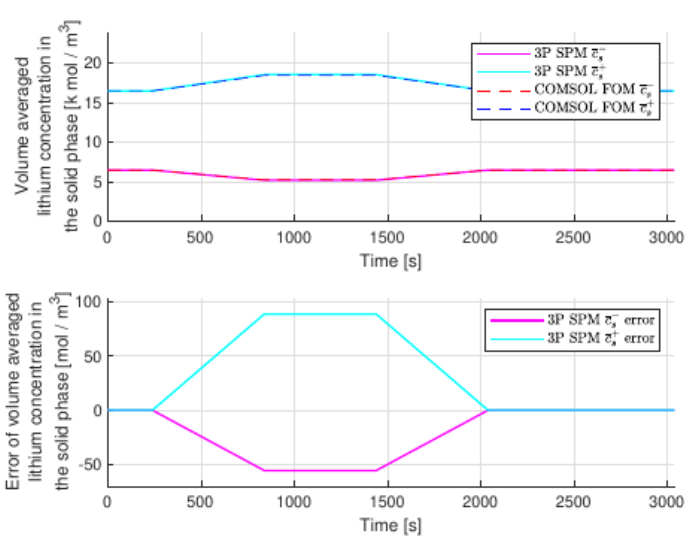
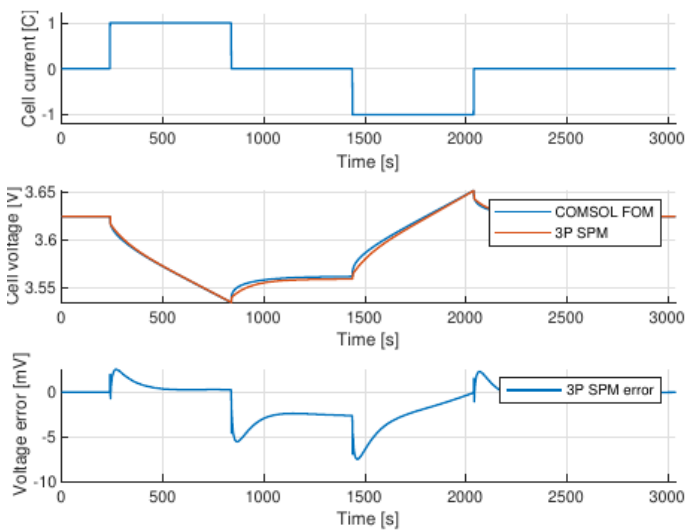
$$c_{ss}(t)$$

$$\dot{x} = Ax + Bu$$
$$y = f(u, x)$$

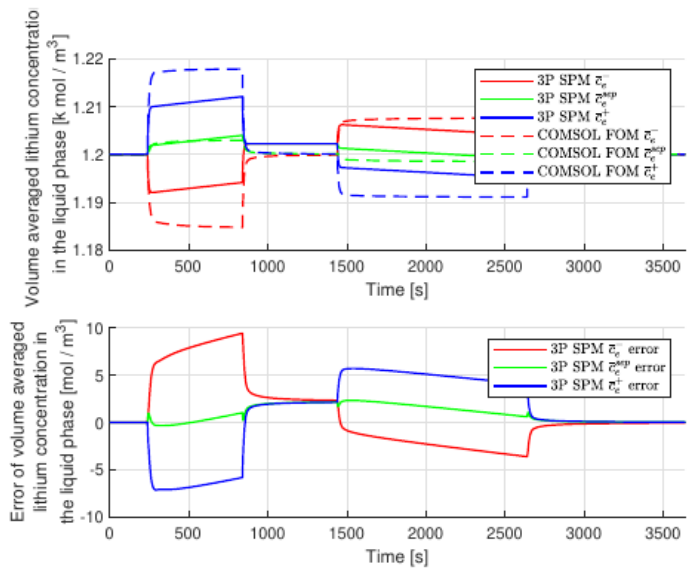
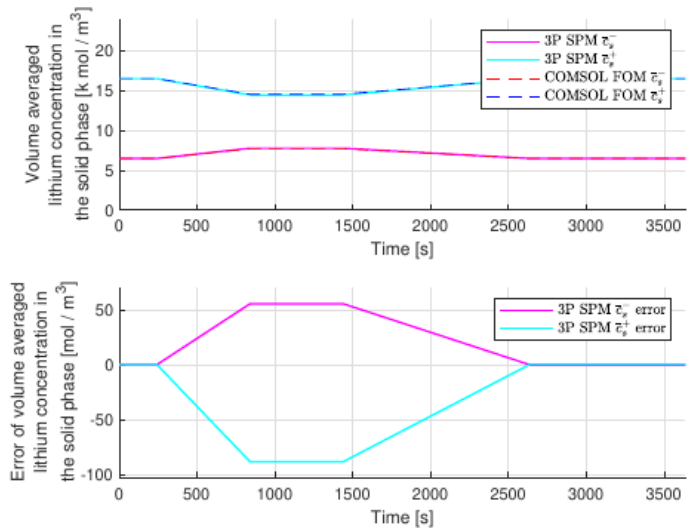
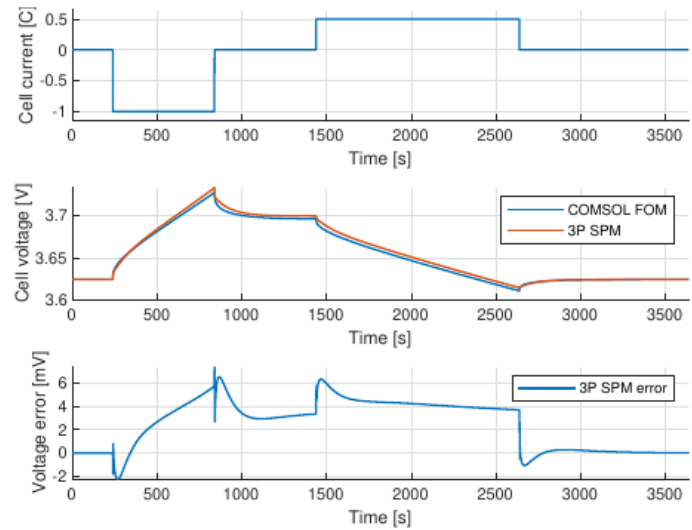


Single Particle Model (SPM) Validation

1C discharge (10min)
1C charge (10min)

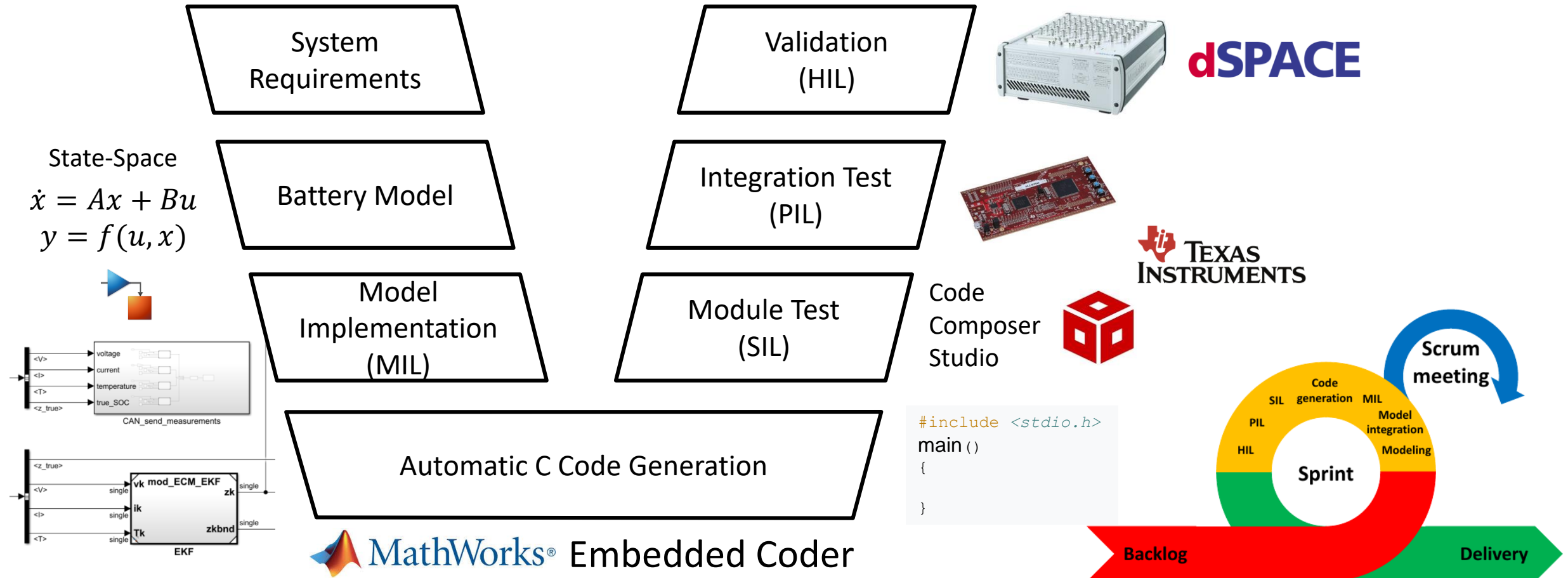


1C charge (10min)
0.5C discharge (20min)



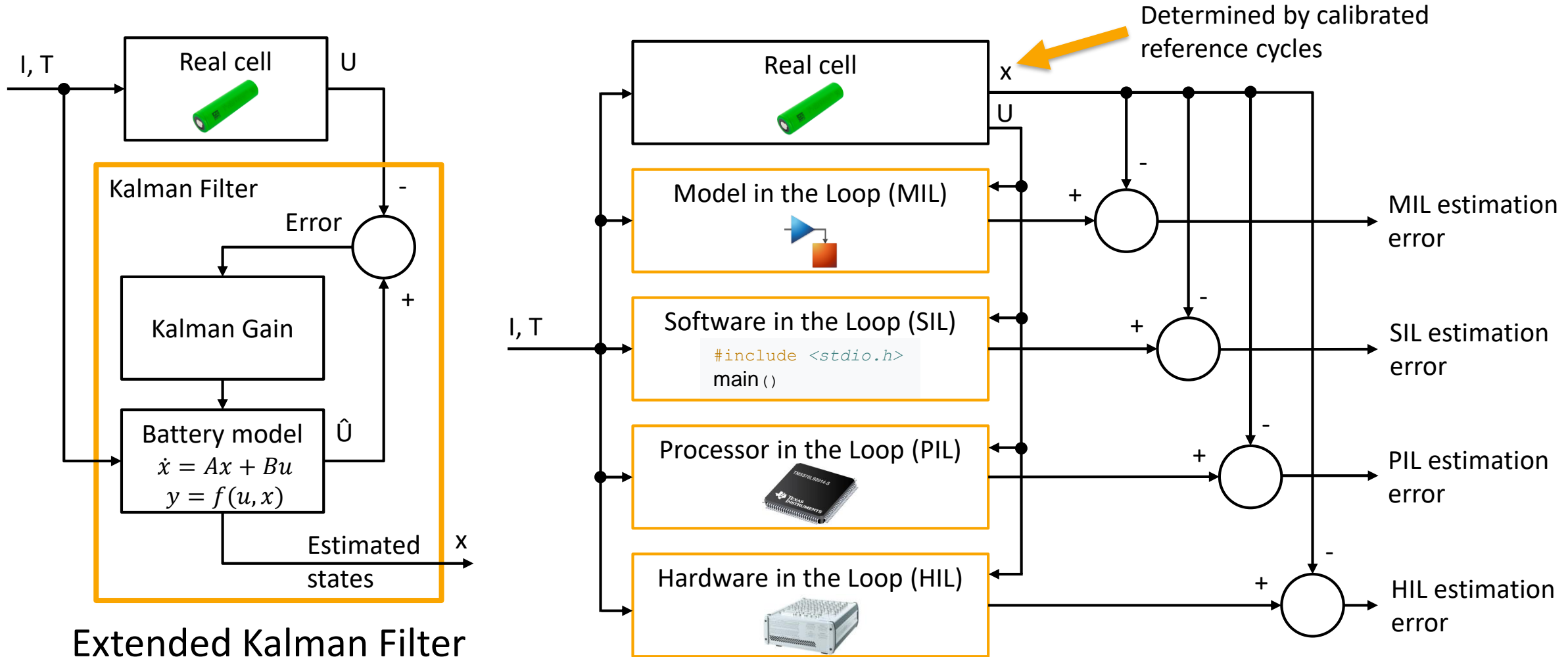
Implementation on an Embedded System

Model-Based Design (MBD)



Implementation on an Embedded System

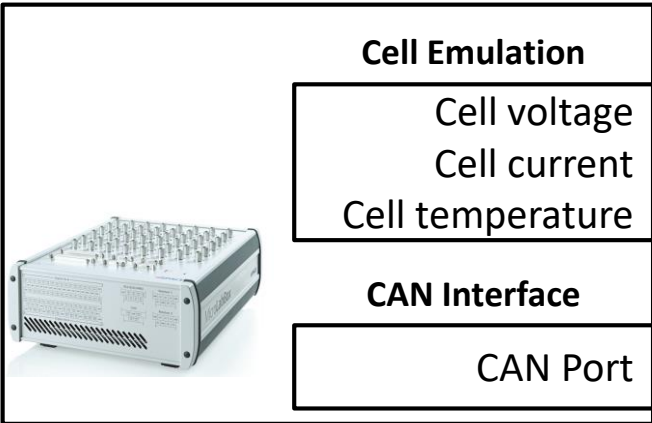
Combination of the battery model and Extended Kalman Filter (EKF)



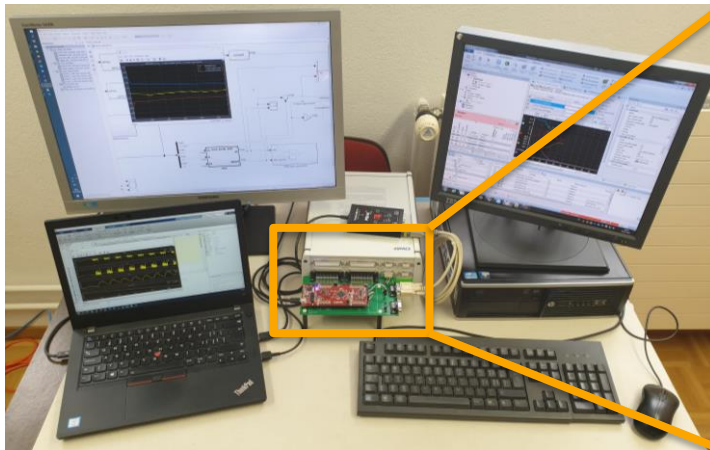
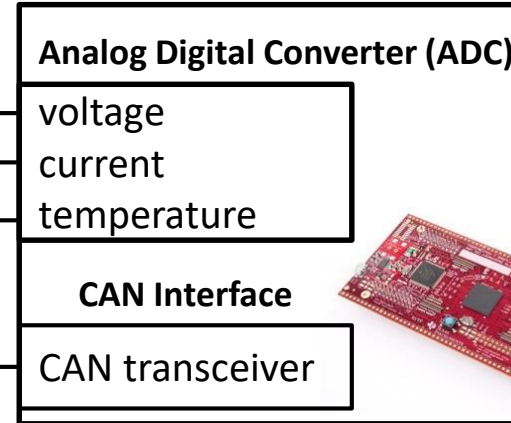
Results of Algorithm Validation

Hardware in the Loop (HIL)

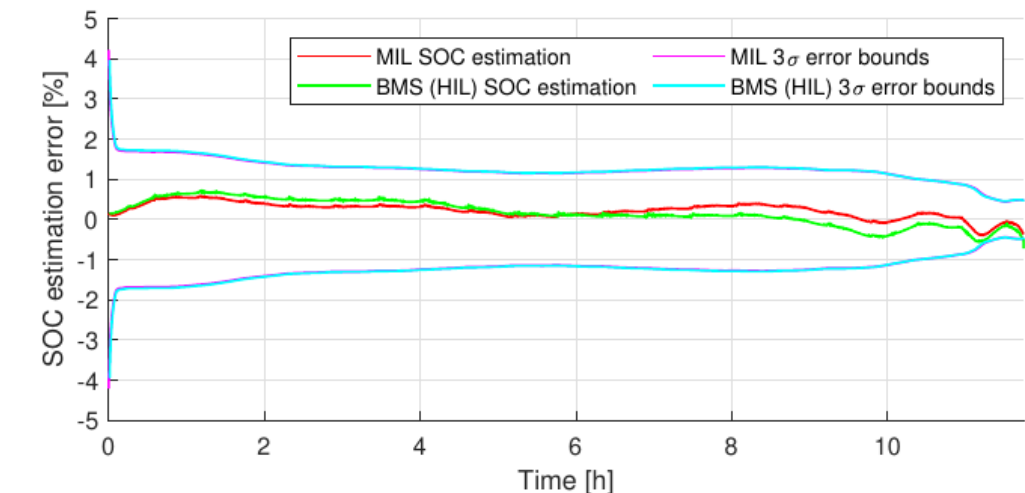
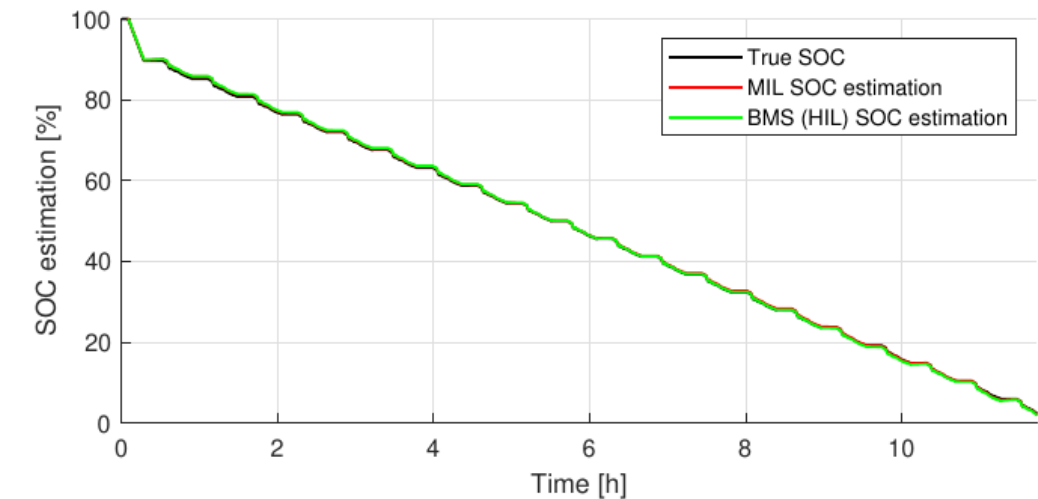
dSPACE MicroLabBox



TI LaunchPad



UDDS drive cycle



Conclusions

- ▶ Successful implementation of a physics-based battery model.
- ▶ Parameter identification of a commercial Li-ion battery.
- ▶ Further improvements of the SPM with electrolyte dynamics are necessary.
- ▶ Achieved model accuracy is comparable with publications from 2018.

- ▶ High demands on batteries and Battery Management Systems (BMS) in Battery Electric Vehicles (BEV) regarding performance, range and safety.
- ▶ Physics-based battery models are expected to become the key technology in advanced BMS due to their ability to estimate electrochemical states and thus allow fast charging and control degradation processes to maximize battery life.